Original Article

Magnetic susceptibility and response time of isotropic and structured magnetorheological elastomers

Barnabás Horváth[1] and **István Szalai**[1,2]

Abstract

The response time of magnetorheological elastomers (MREs) depends on the complex interplay of multiple factors. In this study we investigate the response times of silicone rubber based elastomers containing magnetically soft fillers (iron and magnetite) with isotropic, and two types of anisotropic particle structures. The response times of the elastomers were extracted as the characteristic time constant from the time domain dynamic susceptibility response to ramp excitation in the weak field limit ($H < 10$ kAm^{-1}). The MREs with both types of filler materials in all particle configurations showed a positive susceptibility response, while an inverse proportionality was observed between the response times and the slope of the ramp excitation in all cases. The dynamics of the structural change is found to be highly sensitive to the type of the filler material, and the anisotropy of the microstructure. The response times of the iron loaded MREs varied from (4.0 ± 0.3) ms up to (60.5 ± 2.3) ms. The magnetite loaded MREs displayed faster response (between (1.2 ± 0.1) ms and (12.1 ± 1.8) ms), which is attributed to the cross-linking inhibitor effect of the magnetite particles. The anisotropic particle structure also favors a decreased response time, however the remanence of the particles can modify the structural effect.

Keywords

Response time, magnetic susceptibility, magnetorheological elastomer

1. Introduction

Magnetorheological elastomers (MREs) are magnetoresponsive soft materials (Filipcsei et al., 2007; Wu et al., 2020). They are analogous to magnetorheological fluids (MRFs) in respect to that magnetizable particles (e.g. iron, magnetite) are dispersed in a non-magnetic carrier matrix. If an external magnetic field is applied, then these materials undergo microstructural changes due to dipole-dipole interactions between the particles. But in case of MREs the matrix is an elastic polymer (silicone rubber, polyurethane, thermoplastic, etc.) (Kang et al., 2020), which limits the motion (displacement and rotation) of the particles, in contrast to MRFs. In the latter the carrier phase is a liquid, thus the particles can move freely in a viscous medium.

As the consequence of the microstructural rearrangement the magnetic field induces a change in the macroscopic properties too, which can be viewed as a response to the magnetic stimulus. The rheological, viscoelastic, magnetic, etc. responses of MREs are exploited in numerous technological applications in the field of actuators (Böse et al., 2021), sensing elements (Becker et al., 2018), and mostly in semi-active control

systems for the damping of noise, shock, and vibration (Behrooz et al., 2014; Gu et al., 2016; Hoang et al., 2011; Li et al., 2020b). One key factor influencing the performance and switching characteristics of a device based on a magnetoactive control element is the response time of the magnetoactive material itself, which determines the lower bound of the total system response time. In case of MRFs the material usually reacts faster than other components (magnetic circuits, electronics, etc.), thus it has only a small contribution to the total system response time. On the other hand, under certain circumstances the slower response of a typical MRE would degrade the switching characteristics of the control system, therefore it is essential to

[1]Research Centre for Engineering Sciences, Functional Soft Materials Research Group, University of Pannonia, Veszprém, Hungary
[2]Institute of Mechatronics Engineering and Research, University of Pannonia, Zalaegerszeg, Hungary

Corresponding author:
Barnabás Horváth, University of Pannonia, 10 Egyetem St, Veszprém H-8200, Hungary.
Email: bhorvath@almos.uni-pannon.hu

understand which factors influence the dynamics of the microstructural change, and how it can be enhanced.

Several experimental methods like X-ray tomography (Gundermann and Odenbach, 2014), and other microscopic methods (Chen et al., 2007; Stepanov et al., 2007) are available to study the microstructure, and the motion of the particles in a MRE, but these methods can not capture the dynamics of the microstructural reordering due to limited temporal resolution. There is a direct relation between the structural changes and the change in macroscopic properties, thus the macroscopic response is dictated by, and contains the dynamics of the microscopic processes responsible for the structural reordering. One direct way to characterize the dynamics is to extract the response time from a time domain (TD) macroscopic response (e.g. stress, normal force, magnetization, susceptibility, etc.) recorded during the application of the magnetic excitation by fitting the response with an appropriate model. However, there are only a few studies, which deal with the measurement of the response time of the MREs itself. Zhu et al. (2018) used the normal force response under a stepwise excitation in compression mode to determine the response time and correlate it with the magnetic field strength, particle structure, and compressive strain. They have also investigated the response time of MRE in shear mode based on the shear stress response (Zhu et al., 2019).

In a previous study (Horváth et al., 2022) we have described a measurement method to extract the response time from the TD susceptibility response. We demonstrated the viability of the method by measuring the response times of various MRFs and magnetic fluids, and correlated those with the characteristic time scales of the microscopic processes behind the susceptibility response. It was shown that the susceptometric technique has a high temporal resolution (down to $\sim$1 μs), and enables to record directly the dynamics of the magnetic response. This is important for applications of MREs where the induced change in magnetic properties is exploited (e.g. sensors), and it is not necessarily the same as the response time determined from a mechanical response. Here, we expand on that study, and apply the susceptometric method to investigate the response time of MREs. The focus is on the most simple case, when the material is exposed only to a weak ($H < 10$ kAm^{-1}) magnetic field, where the nonlinear contribution is negligible, and no external deformation is applied to the MRE. The main objective of this study is to make a qualitative picture on how the response time of MREs is influenced by the type of the loading material, the anisotropy of the microstructure, and the magnetic field strength.

2. Experimental

2.1. Measurement of the susceptibility response

Detailed description of the measurement method used for the detection of the TD susceptibility response of the MREs, and technical details of the TD susceptometer were given in Horváth et al. (2022). In the followings we outline only the most important aspects of the experimental setup.

Applying this method the real part (in-phase component, χ') of the complex dynamic susceptibility was measured at a fixed frequency, while the material was exposed to an external magnetic field with a field strength H_e. The susceptibility was determined from the frequency change of an AC probing field with low intensity ($H_{m0} = 0.016$ kAm^{-1}, $f_m \simeq 1$ MHz), which was generated by an LC oscillator inside an air core solenoid (detection coil L). The sample was placed inside the detection coil, so the inductance of L determined the frequency of the sinusoidal probing field (together with the fixed C capacitive element). Therefore, the change in the susceptibility of the sample modulated the frequency f_m of the probing field, which was measured over time t. Due to the geometry of the detection coil the change in susceptibility was always measured along the long axis of the samples (in the z-direction, parallel with the long axis of L, see Figure 1), which gave the z-component of the susceptibility. In the following by the susceptibility χ' we mean always the z-component (this will be relevant in case of the anisotropic MREs, where the susceptibility in different directions are not equal). We define the susceptibility response as the change relative to the initial ($t = 0$) zero field ($H_e = 0$) susceptibility, so $\Delta\chi'(t) = \chi'(t) - \chi'(0)_{H_e = 0}$. The TD susceptometer measures the relative change in susceptibility, thus the initial, zero field AC susceptibility of the elastomers was measured by an inductive method in the frequency range of 500 Hz–1 MHz, using a 4284A impedance analyzer (Agilent, USA). $\chi'(0)_{H_e = 0}$ was calculated from the impedance of the empty (air core) detection coil and the impedance when it is filled with the sample.

The external excitation of the TD susceptometer was generated as a uniform driving field by a Helmholtz coil pair. It was placed around the detection coil so, that the direction of the magnetic field vector was parallel with the long axis of the cylindrical MRE samples (Figure 1). The uniformity of the field strength H_e in the volume of the sample was better than 1%, which was measured with a Magnet-Physik FH54 teslameter. For the response time measurements we used ramp excitation with a constant slope, so $H_e(t) = 0$ for $t < 0$, and $H_e(t) = At$ for $t \geq 0$, where $A = \frac{\Delta H_e}{\Delta t}$ is the slope of
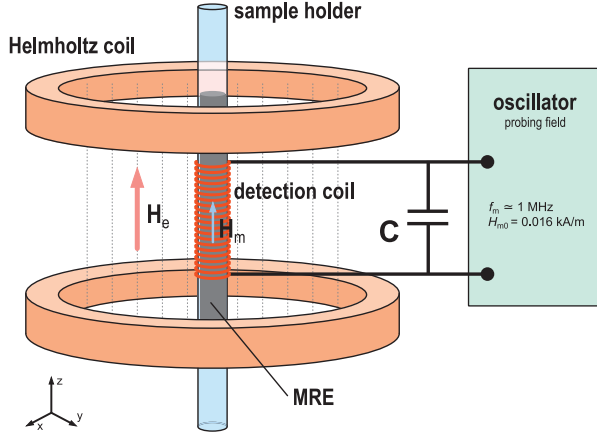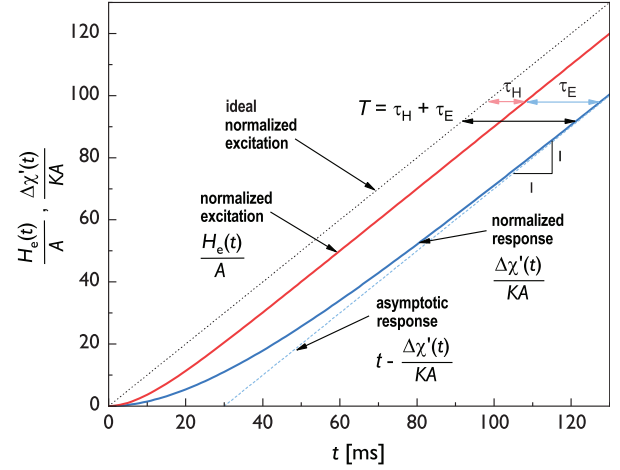
Figure 1. Schematic of the geometrical arrangement during the susceptibility response measurement. The MRE sample fills the detection coil, which is surrounded by the Helmholtz coil generating the external ramp excitation ($\mathbf{H}_e$).

Figure 2. Schematic time domain susceptibility response of the MREs approximated with the response of a first-order system to ramp excitation. In the steady state region the normalized response lags behind the normalized ideal excitation by the time delay T, which is equal to the sum of the lag of the excitation (τ_H) and the response time of the MRE (τ_E). Note that the magnitude of τ_H is greatly exaggerated for demonstration purposes.

the ramp. With the use of a ramp excitation the conditions during real life applications were approached, and the transients associated with the sudden change of the magnetic field were avoided. To investigate the susceptibility response at different rates of excitation the slope of the ramp was varied between 50 kA m^{-1} s^{-1} and 360 kA m^{-1} s^{-1}, by adjusting the duration t_e (in the range of (15–130) ms) and/or the maximum field strength (up to $H_e = 6.5$ kA m^{-1}). The maximum of H_e was limited to remain well below the value required to approach saturation, so the susceptibility response of the investigated MREs would remain in the linear region. We note that the maximum of the magnetic field strength in our experiments was smaller than the values used in typical applications (10–200 kA m^{-1} or even larger). The time delay of the ramp excitation introduced by the inductance of the Helmholtz coil pair (which can be viewed as a series RL circuit) is determined by the L_H inductance and the R electrical resistance of the circuit as $\tau_H = \frac{L_H}{R}$. This time delay can be regarded constant in the range of the current ramps and had a value of $\tau_H = 0.9$ ms. The response times of the MREs were corrected with τ_H as described in the next section.

2.2. Determination of the response time

The method used for the extraction of the response time of the MREs from the TD susceptibility is outlined in the following.

$\Delta\chi'(t)$ is approximated by the response of a first-order linear system to ramp excitation with a slope of A. After the initial transient period ($t \gg T$) the steady state is reached, where $\Delta\chi'(t)$ is close to linear and lags behind the ideal excitation by a time delay T. So $\Delta\chi'(t) = KA(t - T)$, where K corresponds to the steady state gain of the system. To ensure that the response

reached the linear steady state region the length of the recorded response had to be longer than $4T$.

To determine the response time of the MRE the time delay T was calculated. For that the response was scaled by KA, so the linear steady state region had a slope of unity, which was fitted by linear regression to obtain the asymptotic response. The time delay was calculated from the asymptotic response as $T = t - \frac{\Delta\chi'(t)}{KA}$.

Because the ramp excitation was not ideal, but had a $\tau_H = 0.9$ ms lag, the time delay was actually the sum of the time constants of the two sub-processes. The first-order responses of the electromagnetic circuit and the MRE connected in series yielded an overall steady state time delay $T = \tau_H + \tau_E$, where the time constant τ_E was defined as the response time of the MRE (Figure 2).

The response curves were recorded in triplicate. The corrected response times were determined from each curve, and their average together with the standard deviations were calculated. The latter were used to generate error bars.

2.3. Materials

We have investigated the response times of MREs which contained different magnetizable particles in silicone rubber (polydimethylsiloxane, PDMS) matrix. The elastomer matrix was Elastosil RT604 A/B addition-curing, two component silicone rubber by Wacker. Component A contained the platinum catalyst, while the crosslinker was in component B.

As the filler material iron (Fe(0)) and magnetite (Fe_3O_4) particles were used. As the iron filler Nanofer

Star by Nano Iron was used, which is an air-stable, zero valent iron powder (nFe). The surface stabilized nano-particles had a nominal core diameter of 60 nm. At this size the iron particles are magnetic multi domains. The thickness of the stabilizing oxide layer was ~4 nm. The relative iron content of the material was 74% by mass, besides the mixture of iron oxides. The particles formed clusters and agglomerates in the powder form, therefore it was necessary to disperse the agglomerates before the preparation of the MREs (see next section). The magnetite filler material was Bayferrox 318 M (Lanxess) synthetic iron oxide (bM). The dominant size of the magnetite particles was ~200 nm. Magnetite particles at this size are composed of multiple magnetic domains.

2.4. Preparation of MREs

The composition of the fabricated MREs is summarized in Table 1. The nFe filler material was ground for 4 h to disperse the aggregates in a high speed micro mill (Retsch, Germany) with agate mortar and pestle. The bM magnetite powder was used as supplied. The loading material was added to component A of the silicone rubber. After homogenizing the mixture, component B was added. All prepared MREs had a solid loading of 30.5% by weight, while the concentration of component A and B of the silicone rubber was 65.3% and 4.2% by weight in all cases. The mixture of the silicone rubber components and the filler particles was homogenized again by manual stirring with a glass rod. The air bubbles were removed under vacuum (5 min at a pressure of 300 Pa). The liquid MRE was filled into cylindrical glass tubes with a length of 80 mm and an inner diameter of 3.05 mm. The glass tubes also served as sample holders for the cured MREs during the susceptibility measurements. The length of the samples (80 mm) was significantly larger than the length of the detection coil (25 mm).

Three types of MREs were prepared in case of both filler materials: an isotropic (*I*), where the particles were randomly dispersed in the elastomer matrix; and two structured, anisotropic MREs with parallel (*P*) or perpendicular (*O*) oriented particle chains (in respect with the long axis of the cylindrical samples). The schematics of the structure of the prepared MREs are shown in Figure 3. The anisotropic elastomers were cured in a uniform DC magnetic field ($H = 240$ kAm^{-1}), between the poles of a vertically, and a horizontally mounted iron core electromagnets (VEB Polytechnik, Phylatex, Germany). In both cases the sample holders were placed in the electromagnets with their long axis parallel with the direction of gravity. The magnetic field was applied until the MREs were fully cured. The pot life of the mixtures at room temperature was approximately 1.5 h, but in order to minimize the sedimentation of the particles the curing process was accelerated by heat treatment. The samples were heated to $T = 80°C$ with a hot air blower, so the curing time was reduced to ~ 15 min.

3. Results and discussion

The particle structure and the type of filler material influence not just the dynamic susceptibility response and the response time of the MREs, but those have an effect on the zero field AC susceptibility too. Before the discussion of the response time measurement results, we will examine the correlation between the particle structure and the zero field susceptibility.

### 3.1. Structure and dynamic susceptibility in the zero field limit

The morphology of the MRE microstructure is analyzed using representative cross-sectional scanning electron microscopic (SEM) images taken with an Apreo SEM (Thermo Fisher, USA) at an acceleration voltage of 20.0 kV.

The SEM images in Figure 4 show the parallel (Figure 4(a) and (c)) and perpendicular (Figure 4(b) and (d)) cross sections of the same particle structure, when the elastomers with different filler materials were cured in a magnetic field parallel with the samples' long axis (orientation *P*). It is clear that these MREs have an anisotropic structure: adjacent particles form chain like structures, such as densely packed columns and filaments along the direction of the magnetic field. These structures with varying length are highly irregular in shape and meander through the elastomer matrix.

Table 1. Composition of the fabricated MREs.

Sample	Structure	Filler type
nFe MRE-I	isotropic	Fe
nFe MRE-O	anisotropic perpendicular	Fe
nFe MRE-P	anisotropic parallel	Fe
bM MRE-I	isotropic	Fe_3O_4
bM MRE-O	anisotropic perpendicular	Fe_3O_4
bM MRE-P	anisotropic parallel	Fe_3O_4

The concentration of component A and B of the silicone rubber was 65.3% and 4.2%, with a solid loading of 30.5% by weight in all cases.
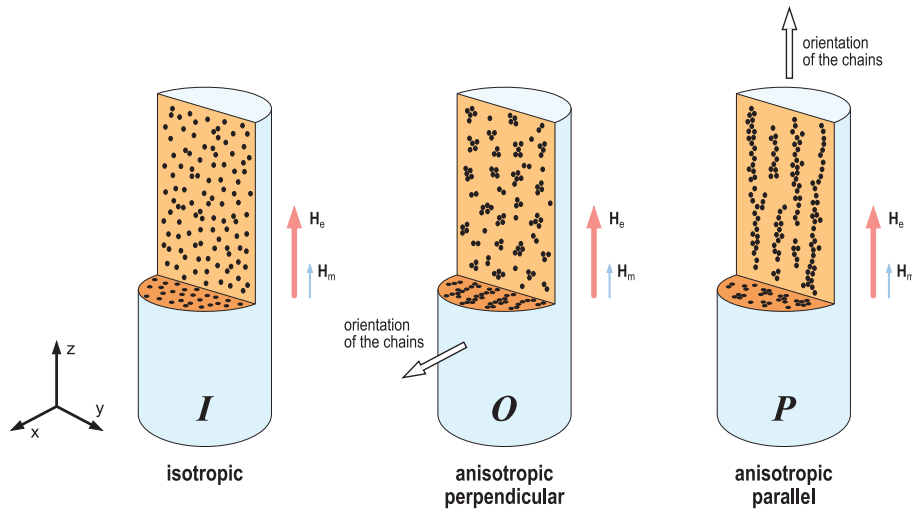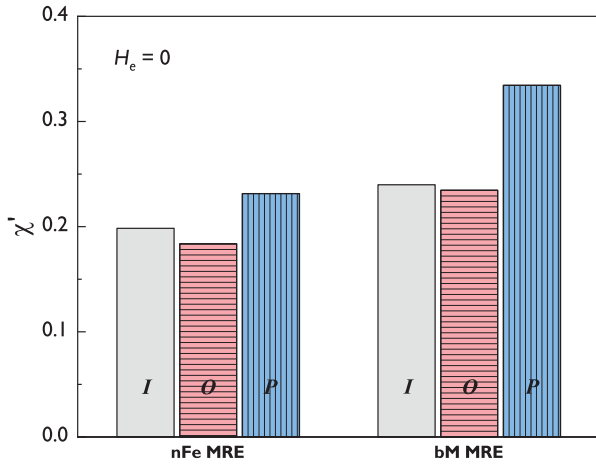
Figure 3. Schematic structure of the isotropic (*I*) and the two configurations of the anisotropic MREs. The orientation of the chain like structures (indicated by the hollow arrows) is perpendicular (*O*) to or parallel (*P*) with the z-axis of the cylindrical samples. The larger arrows show the direction of the driving magnetic field (H_e) during the ramp excitation, while the detection field (H_m) for the susceptibility response measurement oscillates in the direction shown by the smaller arrows. Both magnetic fields are parallel with the z-axis.
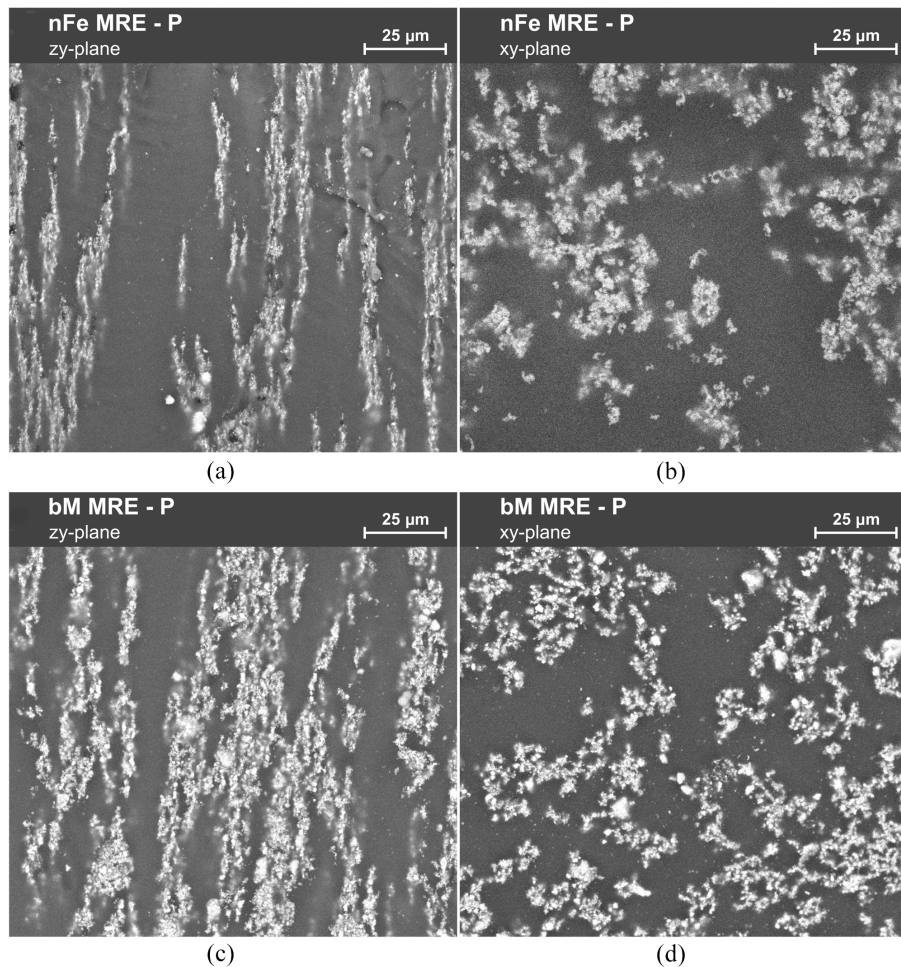
Figure 4. Typical SEM images of the cross section of the elastomers with parallel (orientation *P*) particle chains in case of the nFe iron (a and b) and bM magnetite particle loading (c and d). The left side shows the cross section in the zy-plane (parallel with the chains) and the right side in the xy-plane (perpendicular to the chains).

Figure 5. The z-component of the zero field AC susceptibility (at $f = 500$ Hz) is increasing in case of the *P* oriented chains, while the perpendicular structures (*O*) decrease it compared to the isotropic (*I*) MREs.

Some of them are split, and the branches are attached to neighboring columns, while numerous columns form larger clusters. The cross sections in the xy-plane (perpendicular to the filaments) reveal, that the columns in the clusters are only connected loosely with irregular depleted regions of pure elastomer matrix between them. It was shown by Günther et al. (2012) and Borin et al. (2012) that this structure appears only when the concentration of the particles is above ~25% by mass, and the magnetic field during the curing process is relatively strong ($H > 200$ kA m^{-1}). The size of the columnar structures and the clusters are similar in case of both loading materials. The width of the columns is highly variable, but it is typically around 1–5 μm, while the clusters are much larger and reach a size from 50 μm up to 200 μm.

The MREs cured in a magnetic field perpendicular to the samples' long axis (orientation *O*) also have an anisotropic structure, with a morphology very similar to the *P* oriented structures described above. In the isotropic samples (*I*) the particles are randomly distributed in case of both loading materials. The size of the individual iron and magnetite particles varies greatly (both materials are highly polydisperse). Some degree of aggregation, like globular clusters of multiple particles in the iron, and as well in the magnetite loaded isotropic MREs is observed, despite the homogenization during the preparation. These clusters are present in the anisotropic MREs too, as it can be seen as the larger spots in Figure 4(a) and (d).

Now let us compare the initial, zero field susceptibility (measured at $f = 500$ Hz) of the MREs with different particles, and structural arrangement. The correlation between the structural composition and the susceptibility is shown in Figure 5. The MREs containing bM magnetite had a slightly larger susceptibility

than the iron loaded MRE with the corresponding structure. This is true for all three structural arrangements. For example, in case of the isotropic MREs the bM loaded samples had a susceptibility of $\chi' = 0.240$, while $\chi' = 0.199$ for the nFe MREs. The susceptibility of the structured elastomers (*P* and *O* type MREs) becomes anisotropic. *P* oriented chains increase the z-component of the susceptibility χ', while *O* oriented chains decrease it slightly compared to the isotropic (*I*) samples. This trend is true for both types of particle loading, but with different magnitude. The MREs containing nFe particles with *P* chains display an increase of 0.033 (+ 16.6%), and the *O* chains cause a decrease of 0.015 (−7.4%). The magnitude of the difference in case of the bM MRE samples is 0.095 (+ 39.4%) and 0.005 (−2.2%). According to Kiarie et al. (2022) this tendency is only observable for the initial susceptibility (in the linear region of the magnetization curve, when $H_e \rightarrow 0$). Above a threshold field strength the trend is reversed, and the susceptibility of the MRE along *P* oriented structures is smaller, while for the *O* type it is larger compared to the isotropic case.

It is worth to mention that the above discussed anisotropy of the susceptibility associated with structure formation is present in liquid based field responsive materials too (de Vicente et al., 2002; Wen et al., 1998), since the particle structure of the anisotropic MRE is comparable to the structure of an activated magneto- or electrorheological fluid.

3.2. Susceptibility response of the MREs

Single examples for the TD susceptibility response of the isotropic and anisotropic MREs with nFe and bM particles are compared in Figure 6(a) and (b), respectively. The shown responses were recorded during a ramp with a slope of $A = 50$ kA m^{-1} s^{-1}, which was the lower limit of the used range of A. The responses under a ramp with steeper slope (up to $A = 360$ kA m^{-1} s^{-1}) were similar to the shown curves, and remained in the linear region in all cases. The maximum of H_e at the end of the ramp excitation was smaller than 6.5 kA m^{-1}, which was well below the magnetic field strength required to approach saturation of the magnetization. In this weak field limit the susceptibility response after the initial transient period was linear, and the linear model fitted it very well. The contribution from the nonlinearity of the magnetization in regard of the applied field becomes relevant only at higher field strengths.

The susceptibility of both the iron and the magnetite loaded elastomers were increasing after the application of the external magnetic field ($\Delta\chi' > 0$). A positive susceptibility response was observed in case of every structural configurations (*I*, *O*, and *P* samples). The magnitude of $\Delta\chi'(t_e)$ near the end of the ramp excitation (at $H_e = 5.2$ kA m^{-1}) for the nFe filler was
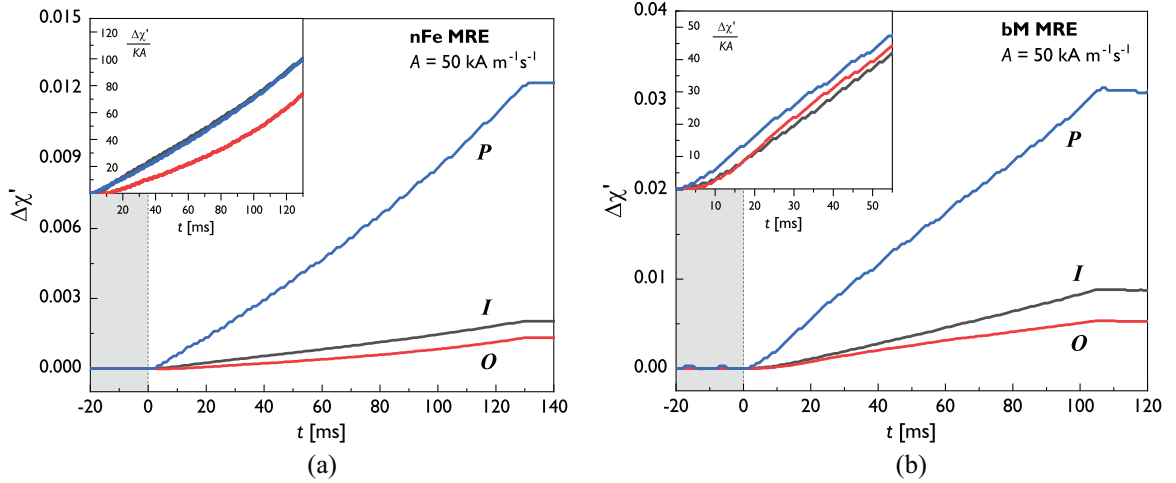
Figure 6. Examples for the TD susceptibility responses of the MREs with different structure to ramp excitation ($A =$ 50 kA m^{-1} s^{-1}) in case of nFe iron (a) and bM magnetite (b) filler materials. The insets show the responses after normalization.

$\Delta\chi'_I = 0.002$, $\Delta\chi'_O = 0.001$, and $\Delta\chi'_P = 0.009$. For the bM loaded MRE samples these values were significantly larger: $\Delta\chi'_I = 0.009$, $\Delta\chi'_O = 0.005$, and $\Delta\chi'_P = 0.031$.

The susceptibility increase of the MREs in an external magnetic field can be associated with the structural changes due to strong dipole-dipole interaction between particles with dipole moments. The extent of the particle motion (i.e. mobility) depends on several factors, but mainly on the rigidity of the elastomer matrix, which constrains the reordering. It is generally accepted that the dipole-dipole interactions reduce the interparticle distances in isotropic and anisotropic MREs as well. In anisotropic MREs chain-chain interactions (which are mostly repulsive) are also present, but play only a minor role (Han et al., 2013). The rearrangement of the particles can be irreversible during the first application of an external magnetic field, causing permanent deformation of the elastomer matrix. After that, during consecutive application of a magnetic field all structural changes are fully reversible. This was shown by several studies (Bodnaruk et al., 2018; Sánchez et al., 2018) at high field strengths, when the elastomers were driven into saturation.

According to our measurements the first irreversible microstructural reordering occurs to some extent even in weak fields, far from saturation. We observed that the susceptibility response during the first ramp excitation ($H_e \leqslant 6.5$ kA m^{-1}) differed from the following ones, which is a sign of the initial irreversible changes. Identical responses were only obtained after consecutive application of the same ramp excitation. The TD response curves in Figure 6 were recorded in such a way, thus these are representative for the fully reversible structural changes.
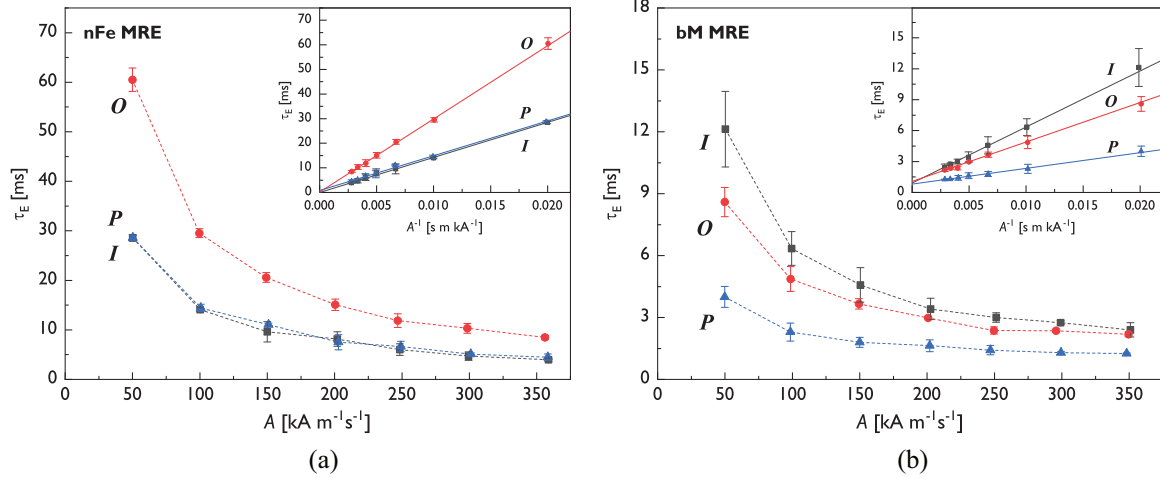
3.3. Response time of the MREs

The macroscopic response times of the MREs were extracted from the TD susceptibility response applying the method described in Section 2.2. The response curves used for this were recorded after the ramp excitation was applied to the sample at least three times, to measure the response time characteristic for the reversible microstructural changes (which are relevant in real life applications).

The response times in case of the two filler particles at different levels of excitation are summarized in Figure 7. The response time τ_E decreases as the slope of the excitation A is increasing. This is true for both filler materials, and for all particle configurations. The dependence is approximately inversely proportional to the slope of the ramp, which is shown by linear regression of the τ_E versus A^{-1} data in the insets of Figure 7. However, there are significant differences in the magnitude of the response times depending on the type of the loading material and the structure of the MREs.

Effect of loading material. The τ_E in case of the nFe loaded elastomers with different structure was between (4.0 ± 0.3) ms and (60.5 ± 2.3) ms (Figure 7(a)). The magnitudes of these values are comparable to the response times of typical MREs (Zhu et al., 2018).

On the other hand, the response time of the bM MREs varied between (1.2 ± 0.1) ms and (12.1 ± 1.8) ms depending on the structural configuration and the slope of the excitation (Figure 7(b)). These response times are substantially smaller than the corresponding τ_E of the elastomers with iron filler. The difference is more conspicuous when a comparison is made between the MREs with the same structure, but

Figure 7. Response time of the nFe (a) and bM (b) loaded MREs in the isotropic (I), and the two anisotropic particle configurations (P and O) depending on the slope of the ramp excitation (symbols). The dashed lines show the trend of the curves. The insets show the linear dependence on the reciprocal of the slope, where the solid lines are linear regressions.
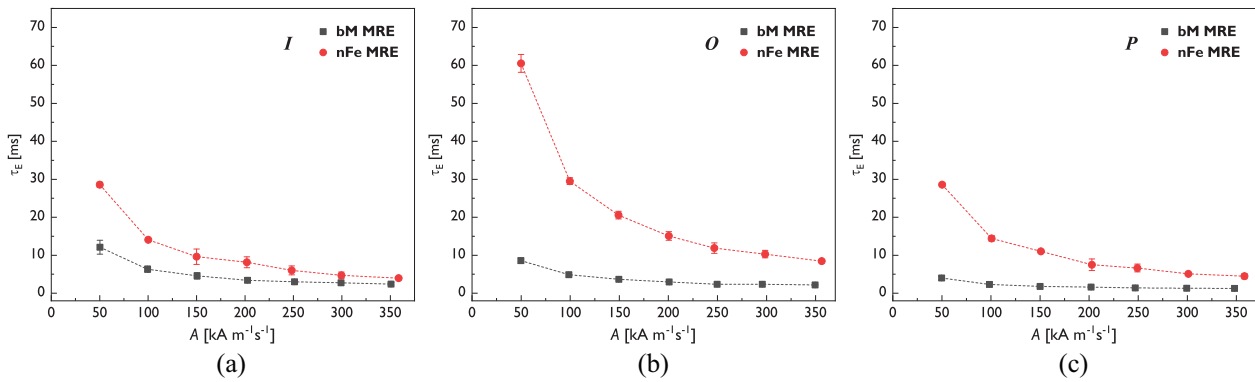
Figure 8. Response time of the isotropic (a) and the anisotropic elastomers with perpendicular (b) and parallel (c) chains in case of the iron (circles) and magnetite (squares) loaded samples. The trend of the curves is shown by the dashed lines.

with different fillers (Figure 8). The response of the bM loaded MREs can be considered fast, even if we compare it to MRFs. The response times discussed here are on the same magnitude as the τ of carbonyl iron based MRFs published in a previous study (Horváth et al., 2022), which were measured by the same TD susceptibility method used here.

It was also observed that the elastic moduli of the MREs with magnetite loading were significantly smaller than the moduli of the pure elastomer regardless of the structural configuration. The elastic moduli (Young's modulus E) of the MREs were measured by static tensile tests in the linear region of deformation. For example, the elastic modulus of the isotropic bM MRE was $E = 55$ kPa, while the pure RT604 silicone rubber had an $E = 663$ kPa. The small response times and the decreased elastic moduli of the bM MREs indicate an incomplete polymerization of the elastomer matrix

around the particles, which decreases the rigidity of the matrix, thus enhances the mobility of the particles. Similar inhibitor effect of the filler particles was pointed out by Borin et al. (2012).

In case of the nFe MREs the curing inhibitor effect of the particles was not observed. The elastic moduli of the nFe MREs were larger (e.g. in the isotropic case $E = 1572$ kPa) than the pure elastomer's, thus the mobility of the iron particles is more constrained, which explains the slower response compared to the bM MREs.

Effect of microstructure. The response time was largely affected by the structural arrangement of the particles in case of both types of loading material. The bM loaded elastomers with parallel chains (P) had the smallest response time: between (1.2 ± 0.1) ms and

(4.0 ± 0.5) ms (depending on the slope of the ramp excitation). Compared to this, the bM samples with perpendicular chains (*O*) showed an increased response time between (2.2 ± 0.1) ms and (8.6 ± 0.7) ms, while the isotropic elastomers (*I*) exhibited even larger τ_E from (2.4 ± 0.3) ms up to (12.1 ± 1.8) ms.

The following qualitative picture can be drawn to explain the structural effects displayed by the bM MREs. The distances between the randomly dispersed particles in the isotropic MRE are larger compared to the structured ones (at the same particle concentration). Thus, due to the distance dependent nature of the dipole-dipole interaction the movement of the particles toward the new equilibrium positions is a slower process in the isotropic configuration. On the other hand, the anisotropic distribution of the particles in the *P* configuration means that the distance between the particles in the direction of the field is reduced. Therefore, due to the stronger dipole-dipole interaction the rearrangement of the microstructure is faster, and τ_E is decreased. Our results correspond to the observations made by Zhu et al. (2018) based on the measurement of the normal force response. Just like our susceptibility response measurements, their normal force response results also support that the response time of anisotropic (containing parallel chains) MRE is significantly smaller compared to the MRE with isotropic structure. Moreover, our results for the anisotropic MREs with perpendicular structures indicate that the configuration *O* also favors a faster response than the isotropic structure. The possible reason behind this is that because the densely packed particle columns form larger clusters (as seen in the SEM images) the interparticle distance in configuration *O* is reduced in the z-direction compared to the isotropic case. Again, the reduced distances result in a faster response. However, since the packing of the columns inside the clusters along the z-axis is not as dense as along the particle columns, the response of the *O* structure is not as fast as in the *P* case. We note that the reduced particle distance in anisotropic MRE affects not just the response time, but the sign and magnitude of the mechanical deformation in a magnetic field as it was reported by Zhou and Jiang (2004), and it has a positive effect on the stiffness and damping performance too (Li et al., 2020a).

In contrast to the bM MREs, the nFe loaded isotropic and anisotropic MREs with *P* structures had nearly identical response times: at the steepest ramp the response times were (4.0 ± 0.3) ms and (4.5 ± 0.7) ms, while in the lower limit of *A* those were (28.6 ± 0.7) ms and (28.6 ± 0.5) ms, respectively. The anisotropic *O* structured nFe MRE showed a significantly larger τ_E from (8.5 ± 0.4) ms up to (60.5 ± 2.3) ms (see Figure 8). One possible explanation of this distinct structural effect of the nFe elastomers could be the different remanence magnetization of the two types of filler particles. The nFe iron and the bM magnetite are soft

magnetic materials, therefore both are easily magnetized in a magnetic field, but the remanence of the iron particles is larger. Thus, in the nFe elastomers the iron particles retained their magnetization after the removal of the external field to a greater extent than the bM particles, which lost nearly all of their magnetization. This was verified by measuring the magnetic flux density around the cylindrical samples with a Hall sensor teslameter (Magnet-Physik FH 54, Germany), which was up to 10 times larger in case of the nFe MREs than in case of the bM elastomers. Due to the larger remanence of the iron filler considerable dipole-dipole interactions could be present between the particles even if the external field is zero. This would have a stiffening effect on the microstructure with different magnitude in case of isotropic and anisotropic MREs, which could alter the dynamics of the response. The exact role of the remanence could be clarified with further investigation conducted on elastomers containing magnetically hard filler, where the remanence of the particles is orders of magnitude larger, thus the effect should be pronounced.

4. Conclusions

The response times of MREs extracted from the TD susceptibility response to external ramp excitation were investigated in the weak field limit. Isotropic and two types of structured MREs based on silicone rubber with magnetite and iron filler particles were fabricated. In summary, the following conclusions were drawn from the obtained results.

- The structure of the MREs influenced the z-component of the zero field susceptibility: parallel oriented chains increased it substantially, while perpendicular structures decreased it compared to the isotropic MRE.
- During the magnetic ramp excitation a positive susceptibility response was obtained in all cases. In the investigated magnetic field strength range ($H_e \leqslant 6.5 \text{ kA m}^{-1}$), far from saturation the responses of the MREs remained in the linear region. The positive response corresponded with the rearrangement and deformation of the microstructure.
- The extracted response times of the isotropic and both anisotropic MREs depended inversely on the slope of the ramp excitation in case of both filler particles.
- The responses of the MREs with magnetite loading were significantly faster compared to the iron loaded MREs, which was attributed to the incomplete polymerization of the elastomer matrix. The inhibited cross-linking of the matrix by the dispersed particles could cause a faster

response, but with that the elastic modulus of the MRE would be also decreased.

- Smaller response times could be achieved with anisotropic MREs (in case of magnetite loading), especially when the anisotropic structure was parallel with the applied field. However, the results for the iron loaded MREs suggested that the remanence of the particles could modify the structural effect.

In this study the simple case without any applied strain was considered. To approach the conditions during real life applications, we plan to investigate the effect of compressive and shear strain on the response time of different MREs with a modified setup in the near future.

ORCID iD

Barnabás Horváth https://orcid.org/0000-0003-3529-446X

References

Becker TI, Zimmermann K, Borin DY, et al. (2018) Dynamic response of a sensor element made of magnetic hybrid elastomer with controllable properties. *Journal of Magnetism and Magnetic Materials* 449: 77–82.

Behrooz M, Wang X and Gordaninejad F (2014) Performance of a new magnetorheological elastomer isolation system. *Smart Materials and Structures* 23(4): 045014.

Bodnaruk AV, Brunhuber A, Kalita VM, et al. (2018) Temperature-dependent magnetic properties of a magnetoactive elastomer: Immobilization of the soft-magnetic filler. *Journal of Applied Physics* 123(11): 115118.

Borin D, Günther D, Hintze C, et al. (2012) The level of cross-linking and the structure of anisotropic magnetorheological elastomers. *Journal of Magnetism and Magnetic Materials* 324(21): 3452–3454.

Böse H, Gerlach T and Ehrlich J (2021) Magnetorheological elastomers — An underestimated class of soft actuator materials. *Journal of Intelligent Material Systems and Structures* 32(14): 1550–1564.

Chen L, Gong XL and Li WH (2007) Microstructures and viscoelastic properties of anisotropic magnetorheological elastomers. *Smart Materials and Structures* 16(6): 2645–2650.

de Vicente J, Bossis G, Lacis S, et al. (2002) Permeability measurements in cobalt ferrite and carbonyl iron powders and suspensions. *Journal of Magnetism and Magnetic Materials* 251(1): 100–108.

Filipcsei G, Csetneki I, Szilágyi A, et al. (2007) Magnetic field-responsive smart polymer composites. In: *Oligomers - Polymer Composites - Molecular Imprinting*. Berlin, Heidelberg: Springer, pp.137–189. DOI: 10.1007/12_2006_104.

Gundermann T and Odenbach S (2014) Investigation of the motion of particles in magnetorheological elastomers by X-μCT. *Smart Materials and Structures* 23(10): 105013.

Günther D, Borin DY, Günther S, et al. (2012) X-ray microtomographic characterization of field-structured magnetorheological elastomers. *Smart Materials and Structures* 21(1): 015005.

Gu X, Li Y and Li J (2016) Investigations on response time of magnetorheological elastomer isolator for real-time control implementation. *Smart Materials and Structures* 25(11): 11LT04.

Han Y, Hong W and Faidley LE (2013) Field-stiffening effect of magneto-rheological elastomers. *International Journal of Solids and Structures* 50(14–15): 2281–2288.

Hoang N, Zhang N and Du H (2011) An adaptive tunable vibration absorber using a new magnetorheological elastomer for vehicular powertrain transient vibration reduction. *Smart Materials and Structures* 20(1): 015019.

Horváth B, Decsi P and Szalai I (2022) Measurement of the response time of magnetorheological fluids and ferrofluids based on the magnetic susceptibility response. *Journal of Intelligent Material Systems and Structures* 33(7): 918–927.

Kang S, Choi K, Nam J-D, et al. (2020) Magnetorheological elastomers: Fabrication, characteristics, and Applications. *Materials* 13(20): 4597.

Kiarie WM, Gandha K and Jiles DC (2022) Temperature-dependent magnetic properties of magnetorheological elastomers. *IEEE Transactions on Magnetics* 58(2): 1–5.

Li S, Liang Y, Li Y, et al. (2020a) Investigation of dynamic properties of isotropic and anisotropic magnetorheological elastomers with a hybrid magnet shear test rig. *Smart Materials and Structures* 29(11): 114001.

Li S, Watterson PA, Li Y, et al. (2020b) Improved magnetic circuit analysis of a laminated magnetorheological elastomer device featuring both permanent magnets and electromagnets. *Smart Materials and Structures* 29(8): 085054.

Sánchez PA, Gundermann T, Dobroserdova A, et al. (2018) Importance of matrix inelastic deformations in the initial response of magnetic elastomers. *Soft Matter* 14(11): 2170–2183.

Stepanov GV, Abramchuk SS, Grishin DA, et al. (2007) Effect of a homogeneous magnetic field on the viscoelastic behavior of magnetic elastomers. *Polymer* 48(2): 488–495.

Wen W, Ma H, Yim Tam W, et al. (1998) Anisotropic dielectric properties of structured electrorheological fluids. *Applied Physics Letters* 73(21): 3070–3072.

Wu S, Hu W, Ze Q, et al. (2020) Multifunctional magnetic soft composites: A review. *Multifunctional materials* 3(4): 042003.

Zhou GY and Jiang ZY (2004) Deformation in magnetorheological elastomer and elastomer–ferromagnet composite driven by a magnetic field. *Smart Materials and Structures* 13(2): 309–316.

Zhu M, Qi S, Xie Y, et al. (2019) Transient responses of magnetorheological elastomer and isolator under shear mode. *Smart Materials and Structures* 28(4): 044002.

Zhu M, Yu M, Qi S, et al. (2018) Investigations on response time of magnetorheological elastomer under compression mode. *Smart Materials and Structures* 27(5): 055017.